

# "Emerging contrasts at ultrahigh fields"

---

A. Dean Sherry

Advanced Imaging Research Center  
Department of Radiology  
UT Southwestern Medical Center

Department of Chemistry & Biochemistry, UT Dallas

ADVANCED IMAGING

AIRC

RESEARCH CENTER

Ultrahigh field NMR and MRI: Science at a  
Crossroads, Nov. 12-13, 2105

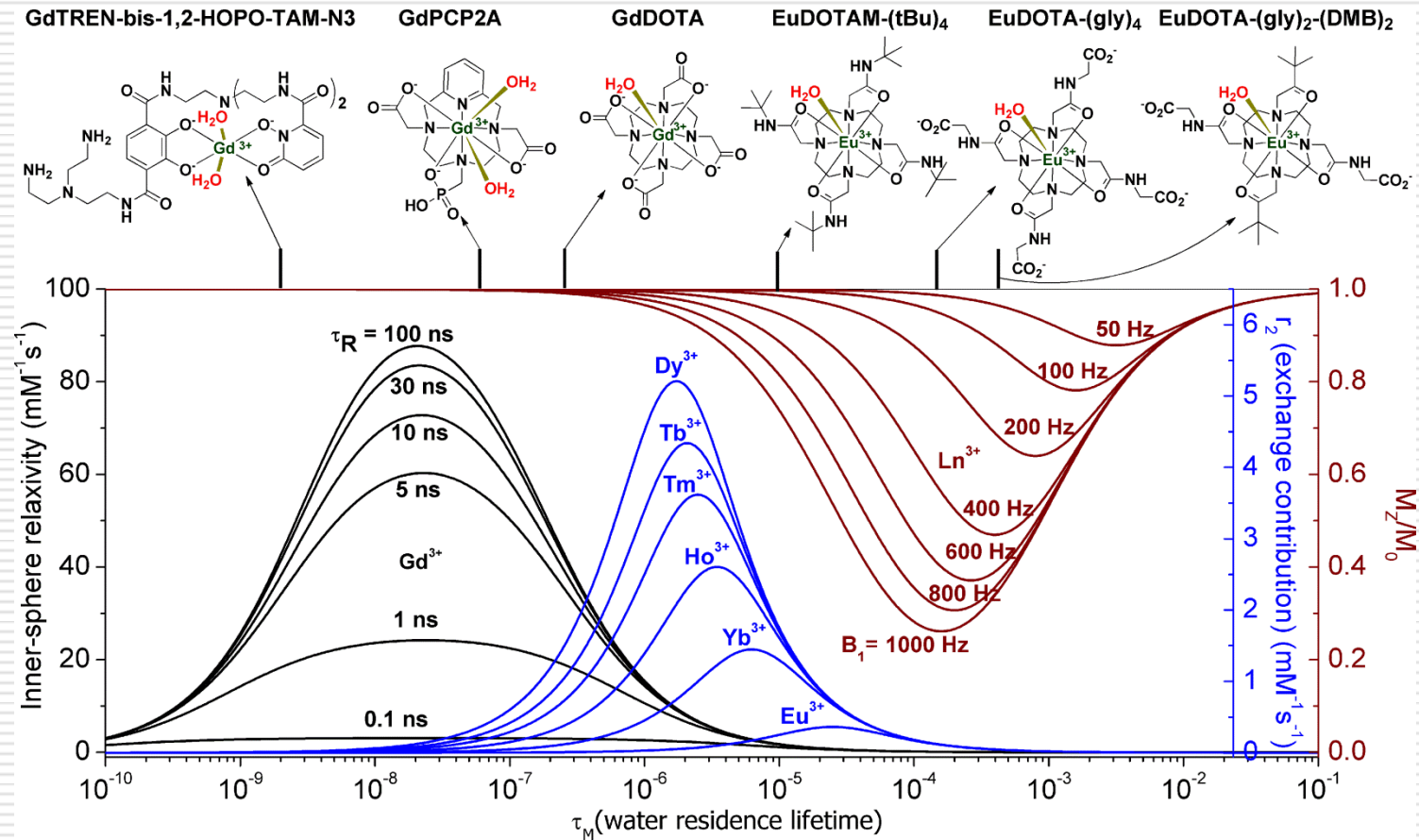
# "Emerging contrasts at ultrahigh fields"

---

- **$T_1$  and  $T_2$  contrast agents**
    - a) Will they remain widely used clinically at high magnetic fields?
  - **Newer types of contrast agents: CEST**
    - a) Opportunities to detect specific cellular metabolites, physiology, and biochemical processes
  - **Spectroscopy of other nuclei**
    - a)  $^{31}\text{P}$ ,  $^{13}\text{C}$  and  $^{23}\text{Na}$  should gain traction as clinical diagnostic tools
-

# The importance of water exchange in the design of MRI contrast agents

AD Sherry & Y Wu, *Curr Opin Chem Biol*, 17: 167-174 (2013).

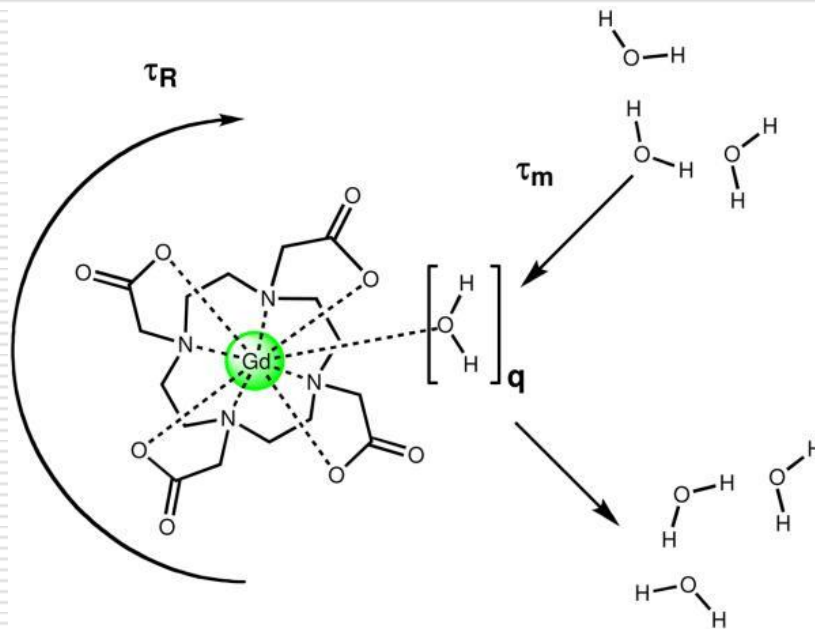


$T_1$  agents

$T_{2\text{exch}}$  agents

PARACEST agents

# Factors to consider in the design of a responsive probe for MRI

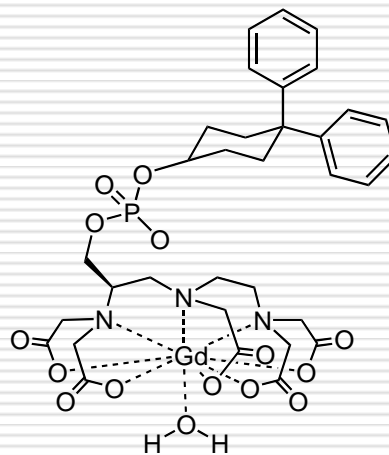
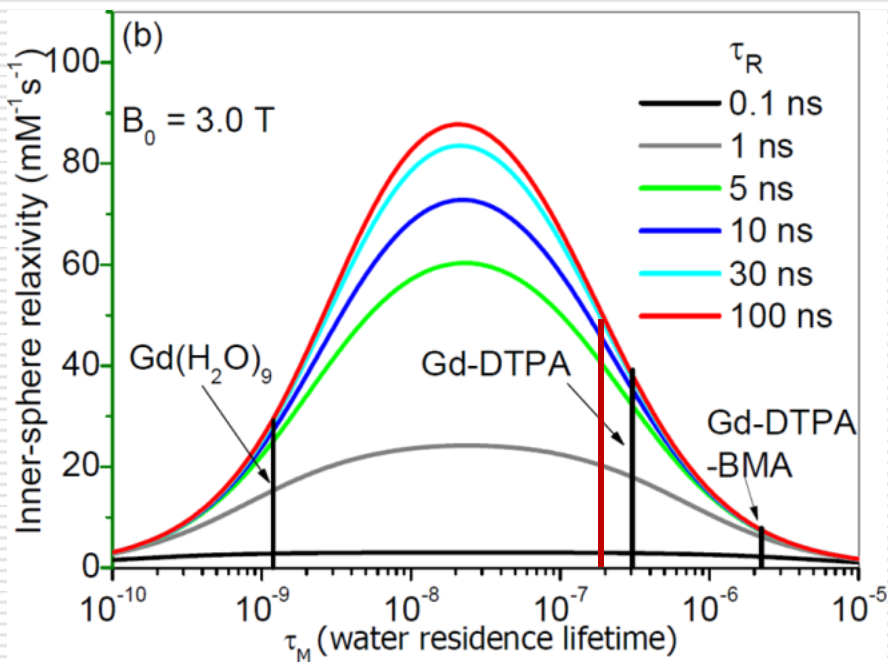


Relaxivity also heavily depends upon the  $Gd-OH_2$  distance ( $r^{-6}$ ) but this is not easily modified.

One of three parameters can be modified:

1. Rotational motion ( $\tau_R$ )
2. Number of inner-sphere water molecules ( $q$ )
3. Water exchange lifetime ( $\tau_M$ )

# The importance of water exchange in the design of MRI contrast agents

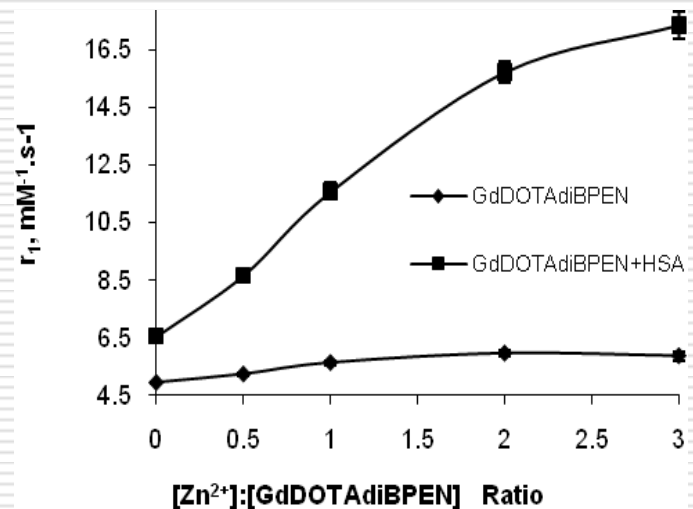
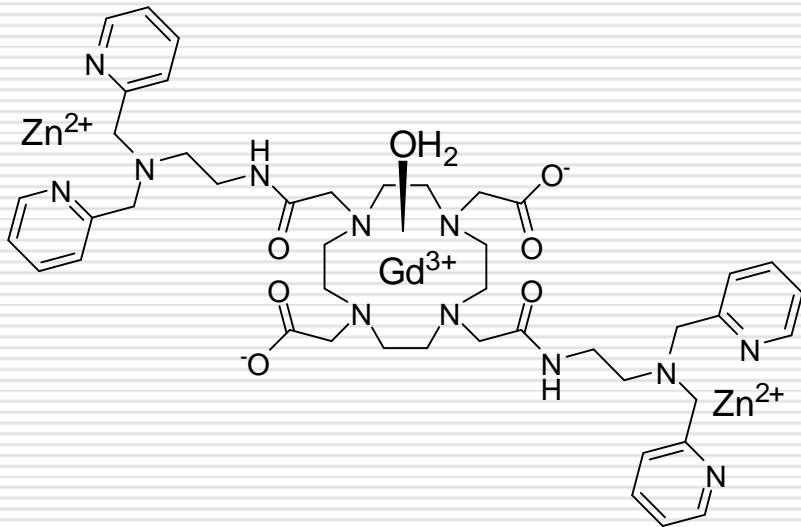


MS-325, Ablavar



MS-325 ( $\tau_M = 172 \text{ ns}$  when bound to HSA)

# Previously reported MRI $Zn^{2+}$ sensors



In the absence of albumin,  
 $r_1$  increases from 5 to 6  
 $\text{mM}^{-1}\text{s}^{-1}$  upon addition of  $Zn^{2+}$

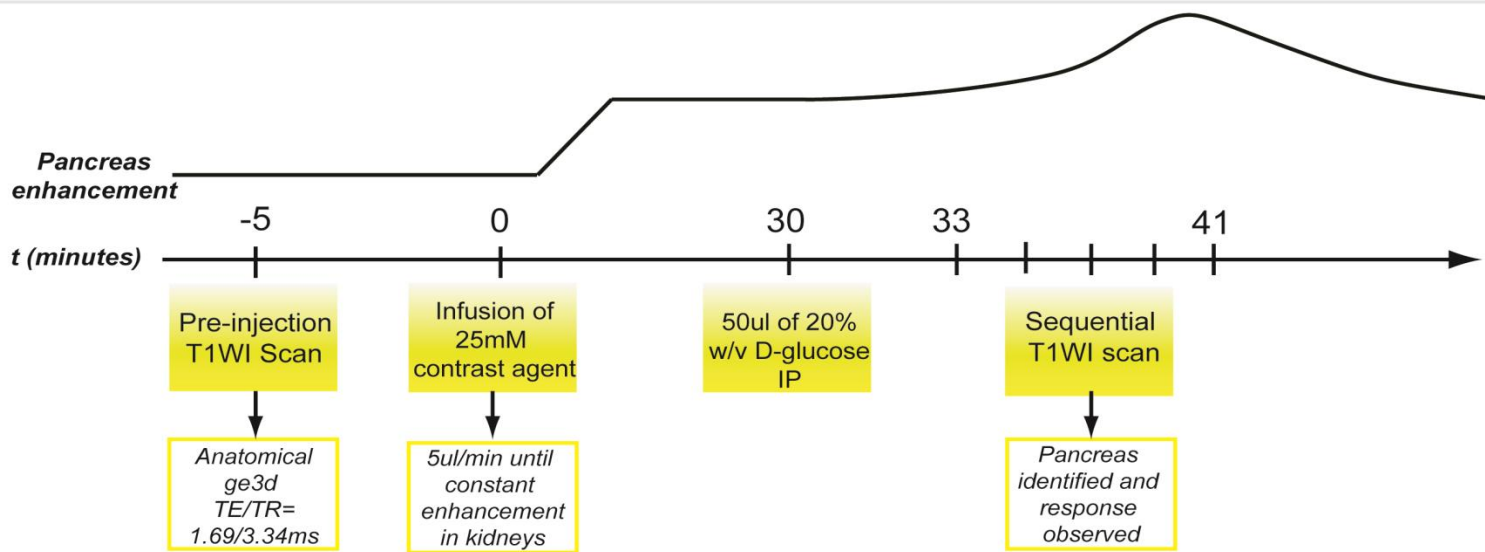
In the presence of albumin,  $r_1$   
increases from 6.6 to 17.5  
 $\text{mM}^{-1}\text{s}^{-1}$  upon addition of  $Zn^{2+}$

$K_d = 5 \text{ nM}$      Positive contrast!

Esqueda, et al., JACS, 131: 11387-11391 (2009)

# The new high relaxivity $Zn^{2+}$ sensors provide much greater image contrast in vivo!

*J. Yu, et al., J. Am. Chem. Soc., 2015, 137 (44), pp 14173-14179*



GdDOTA-diBPEN

Sensor 5

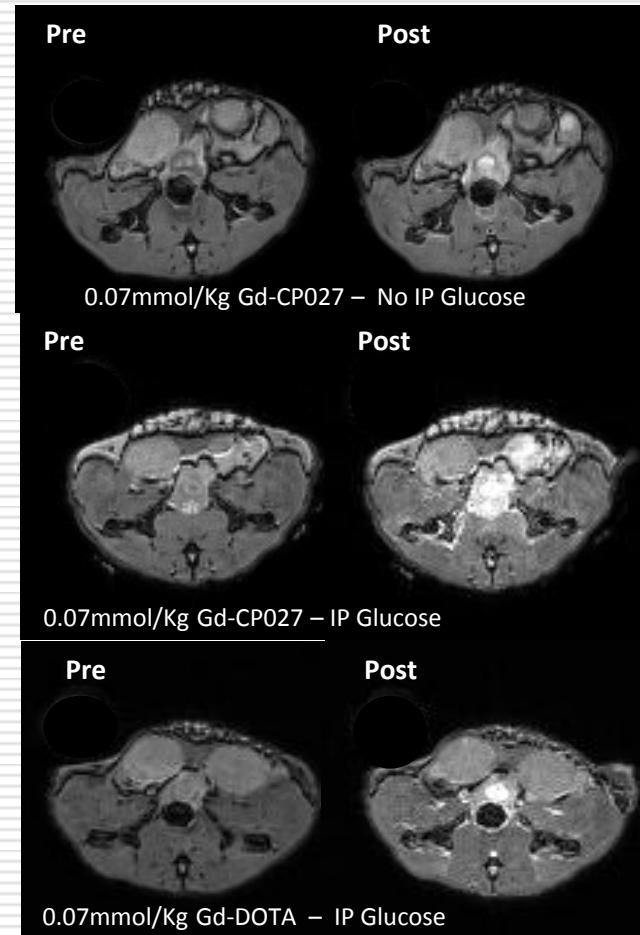
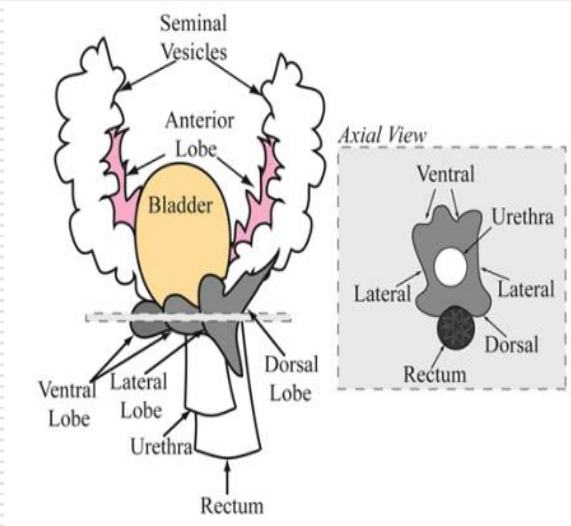
Sensor 4

Gd-HPDO3A

No injection



# Zn<sup>2+</sup> release from the healthy prostate is also stimulated by glucose





# "Emerging contrasts at ultrahigh fields"

---

- Will responsive  $T_1$  agents such as this be useful at higher magnetic fields?
-

# High Magnetic Field Water and Metabolite Proton $T_1$ and $T_2$ Relaxation in Rat Brain In Vivo

deGraaf, et al., MRM, 56: 386-394 (2006)

Table 1  
 Water  $T_1$  and  $T_2$  Relaxation Time Constants for Rat Brain at 4.0, 9.4, and 11.7 T

	Structure								
	cc	cx	ob	hc	cw	cg	st	th	mb
4.0 T									
$T_1$ (ms)	1096.8	1285.8	1640.6	1334.1	1046.9	1352.6	1288.2	1169.4	1064.4
SD (ms)	49.3	77.0	20.8	97.4	53.3	82.6	87.3	69.5	17.3
9.4 T									
$T_1$ (ms)	1752.1	1948.4	2129.1	2059.7	1660.3	2097.2	1927.0	1793.1	1786.5
SD (ms)	52.1	51.9	63.7	66.1	79.3	68.2	54.7	64.3	81.9
11.7 T									
$T_1$ (ms)	1861.3	2073.4	2304.3	2222.8	1745.1	2109.4	2046.5	1903.2	1893.2
SD (ms)	73.5	100.7	63.4	63.2	36.0	95.0	55.3	61.2	44.3
4.0 T									
$T_2$ (ms)	57.9	65.2	80.2	72.0	58.8	65.3	69.7	61.7	60.6
SD (ms)	1.6	2.4	2.0	1.3	1.5	2.0	2.0	2.1	1.9
9.4 T									
$T_2$ (ms)	35.8	42.1	48.1	45.4	37.2	41.7	43.5	40.6	40.3
SD (ms)	1.2	1.2	1.9	1.8	2.0	1.6	2.4	1.2	1.4
11.7 T									
$T_2$ (ms)	30.7	36.2	38.9	38.9	27.1	37.3	36.4	33.8	33.8
SD (ms)	1.0	1.0	1.1	1.3	1.3	2.3	2.2	1.6	1.9

cc = corpus callosum, cx = cerebral cortex, ob = olfactory bulb, hc = hippocampus, cw = cerebellar white matter, cg = cerebellar gray matter, st = striatum, th = thalamus, mb = mid-brain.

$T_1$   
 ~70-80%  
 longer

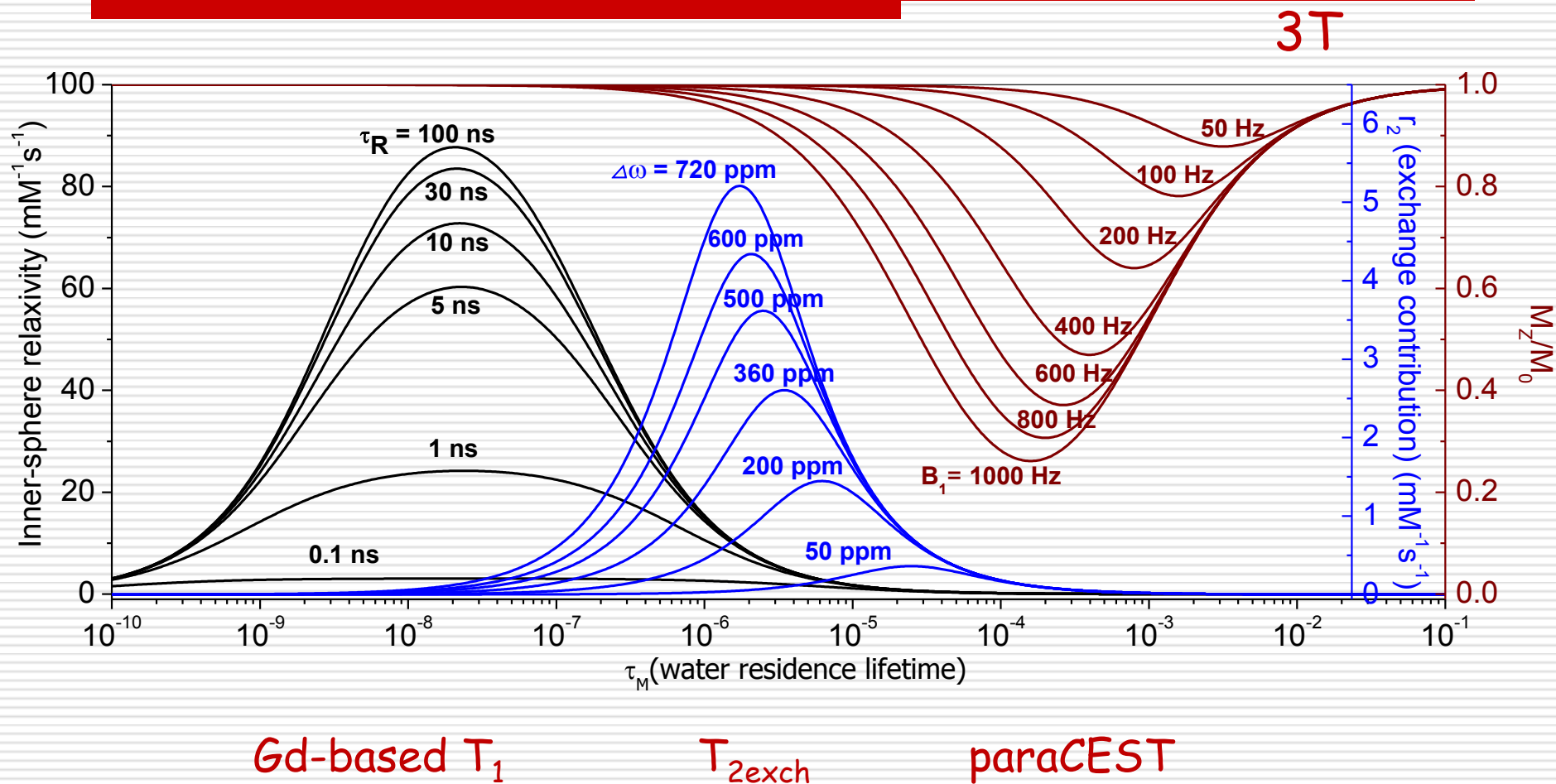
$T_2$   
 ~50%  
 shorter

# Relaxation times measured on the same subjects in human brain (Philips scanners)

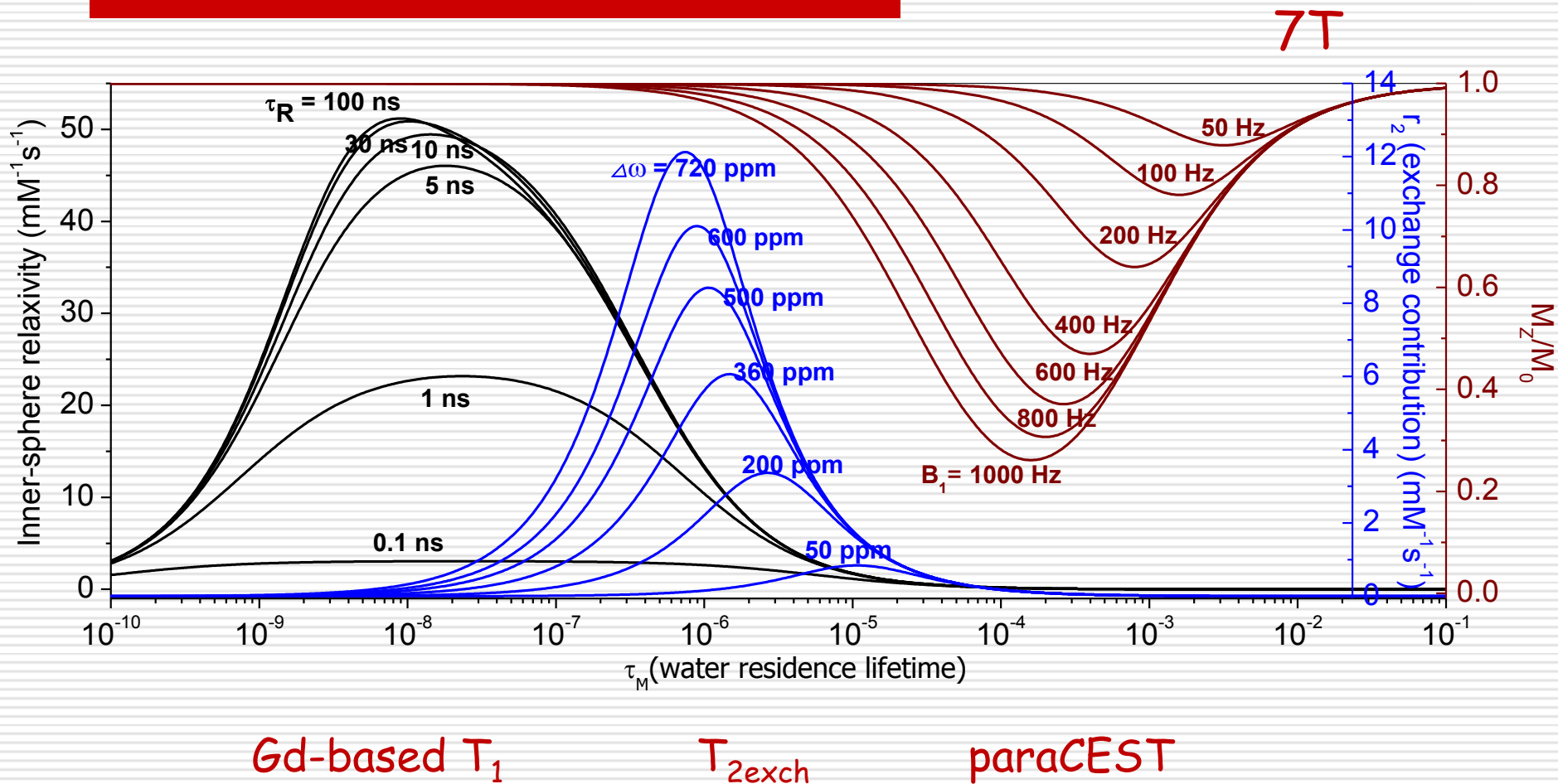
Masaya Takahashi, UTSW, unpublished data

Tissue	T <sub>1</sub> (ms)			T <sub>2</sub> (ms)		
	1.5T	3T	7T	1.5T	3T	7T
<b>Gray Matter</b>						
Frontal cortex	1362	1599	1756	99	91	77
Putamen	1096	1230	1378	80	71	51
Caudate nucleus	1275	1359	1548	87	77	57
Thalamus	1186	1255	1473	82	71	49
Globus pallidus	801	914	1060	71	65	42
<b>White Matter</b>						
Frontal	721	800	914	77	72	61
Corpus Callosum	702	791	965	78	69	54

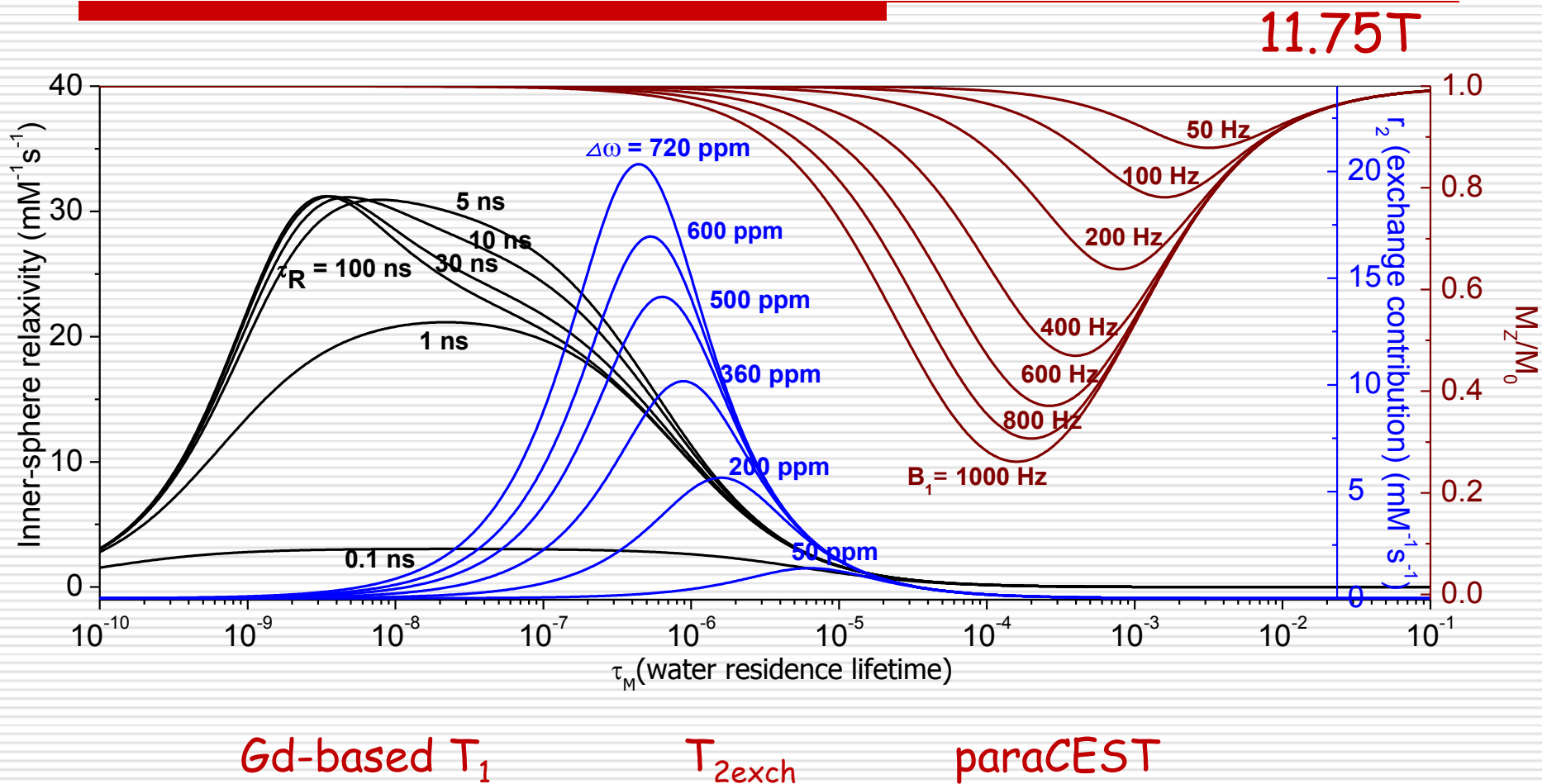
# Impact of water exchange rates on CA sensitivity as one transitions to higher magnetic fields for imaging



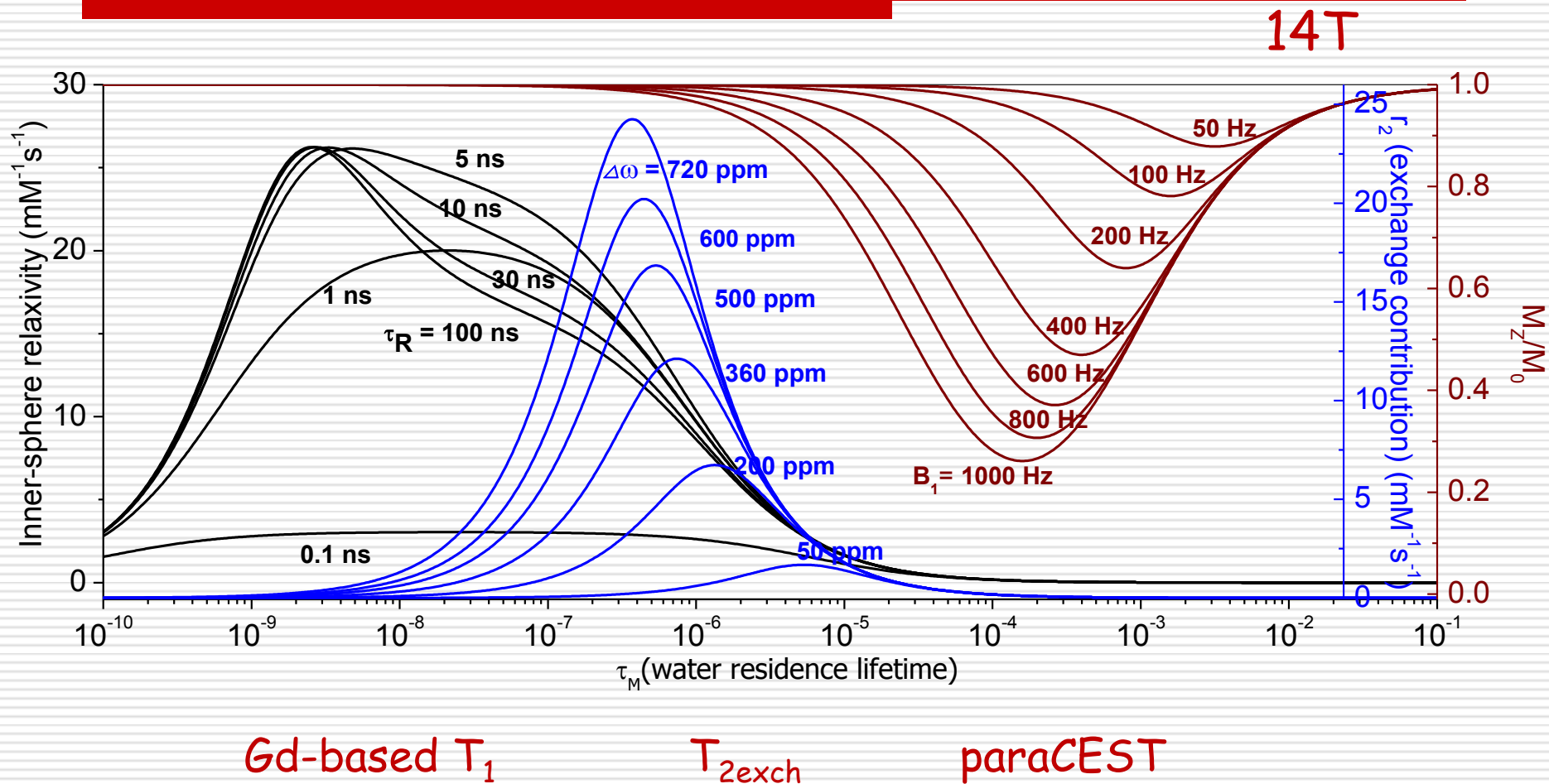
# Impact of water exchange rates on CA sensitivity as one transitions to higher magnetic fields for imaging



# Impact of water exchange rates on CA sensitivity as one transitions to higher magnetic fields for imaging



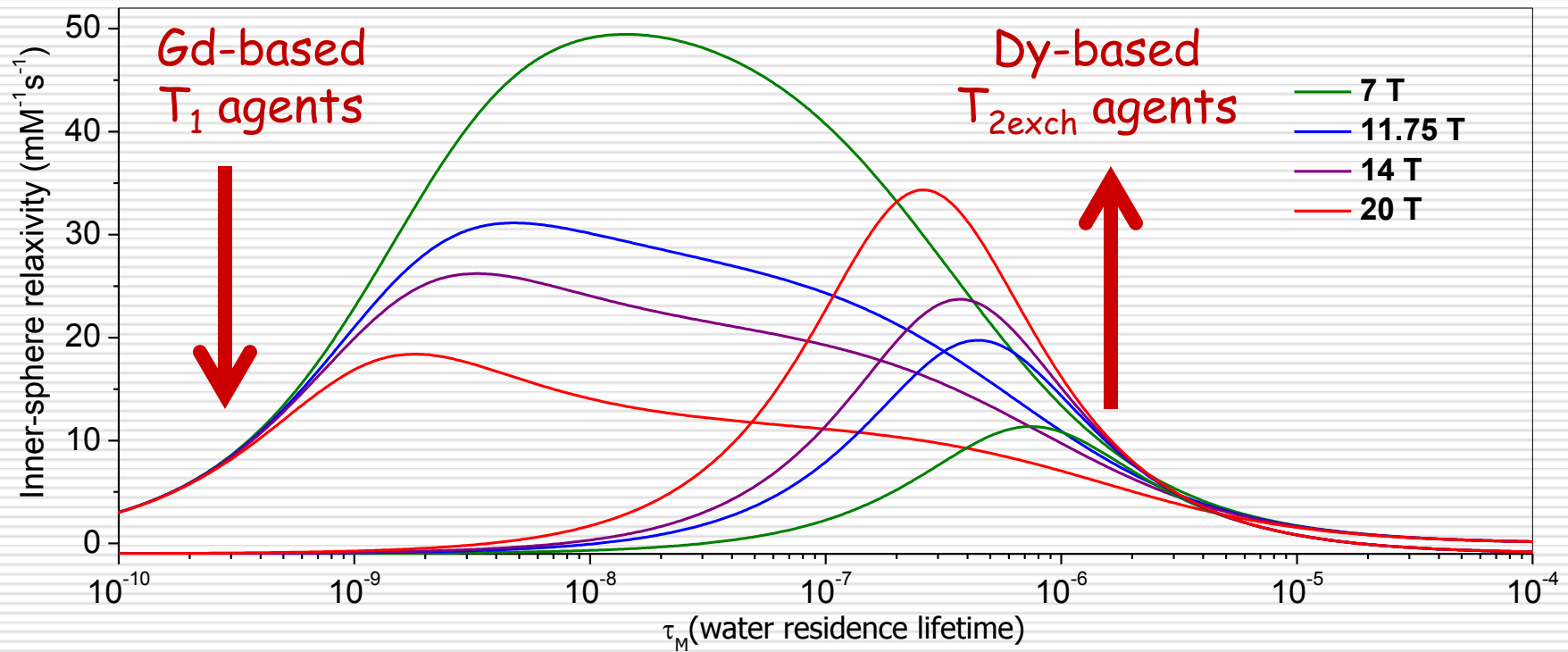
# Impact of water exchange rates on CA sensitivity as one transitions to higher magnetic fields for imaging





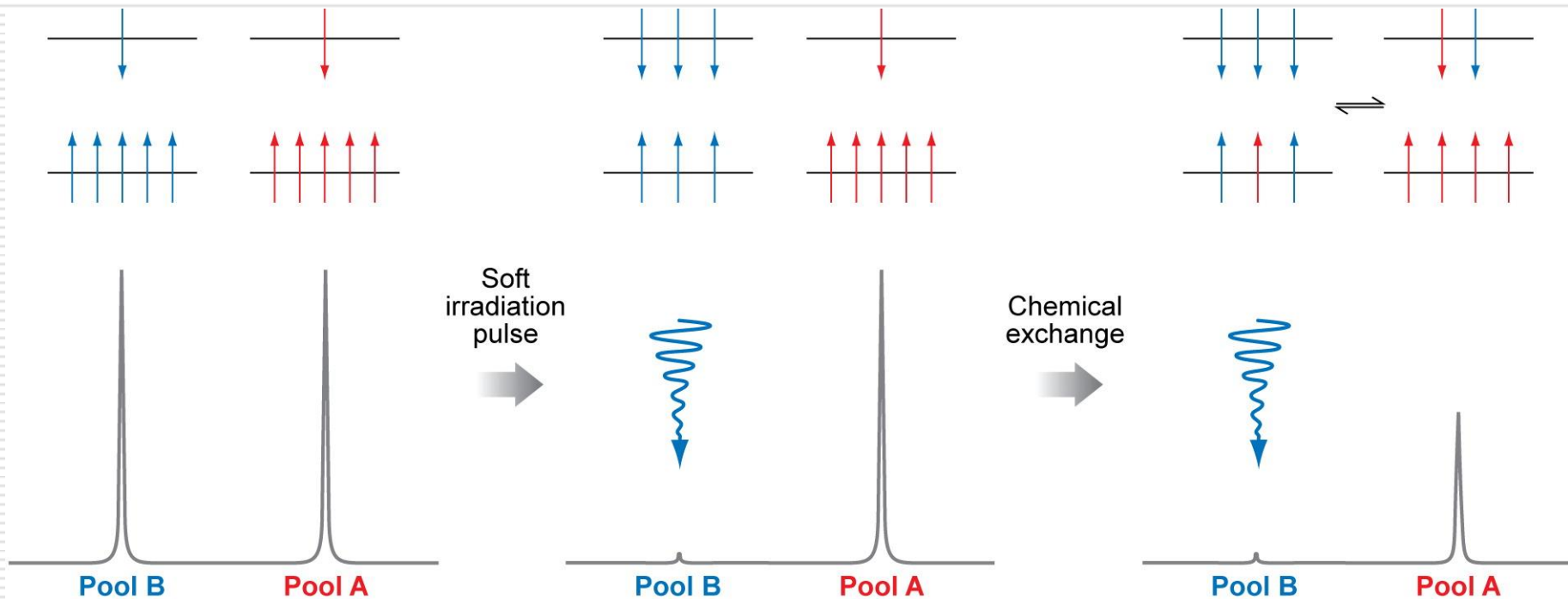
# Impact of water exchange rates on CA sensitivity as one transitions to higher magnetic fields for imaging

plotted on the same  $r_{1,2}$  relaxivity scale



- 
- **Newer types of contrast agents: CEST**
    - a) Opportunities to detect specific cellular metabolites, physiology, and biochemical processes
-

# Basic principles of chemical exchange saturation transfer (CEST) imaging

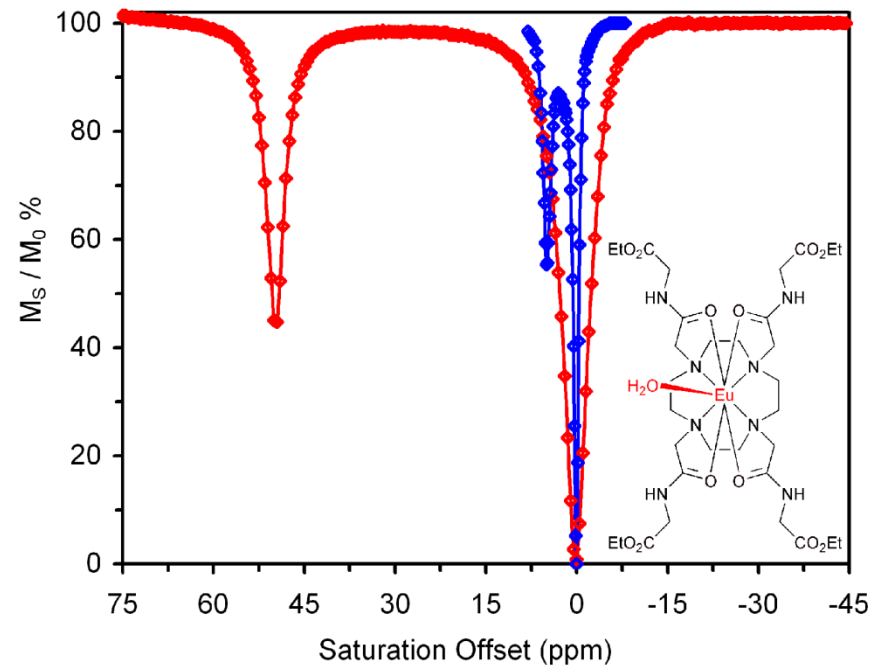
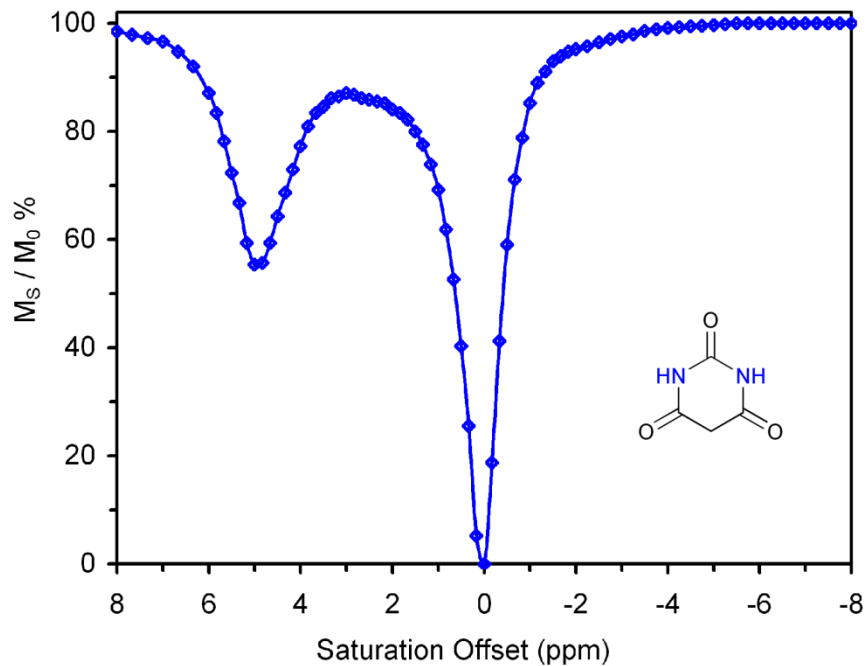


Chemical shift,  $\Delta\omega$ ,  
must differ

RF saturation must  
be selective

Intermediate  
exchange rate,  
 $k_{ex} < \Delta\omega$ ,

# One clear advantage of PARACEST agents for CEST imaging $\Rightarrow$ large $\Delta\omega$

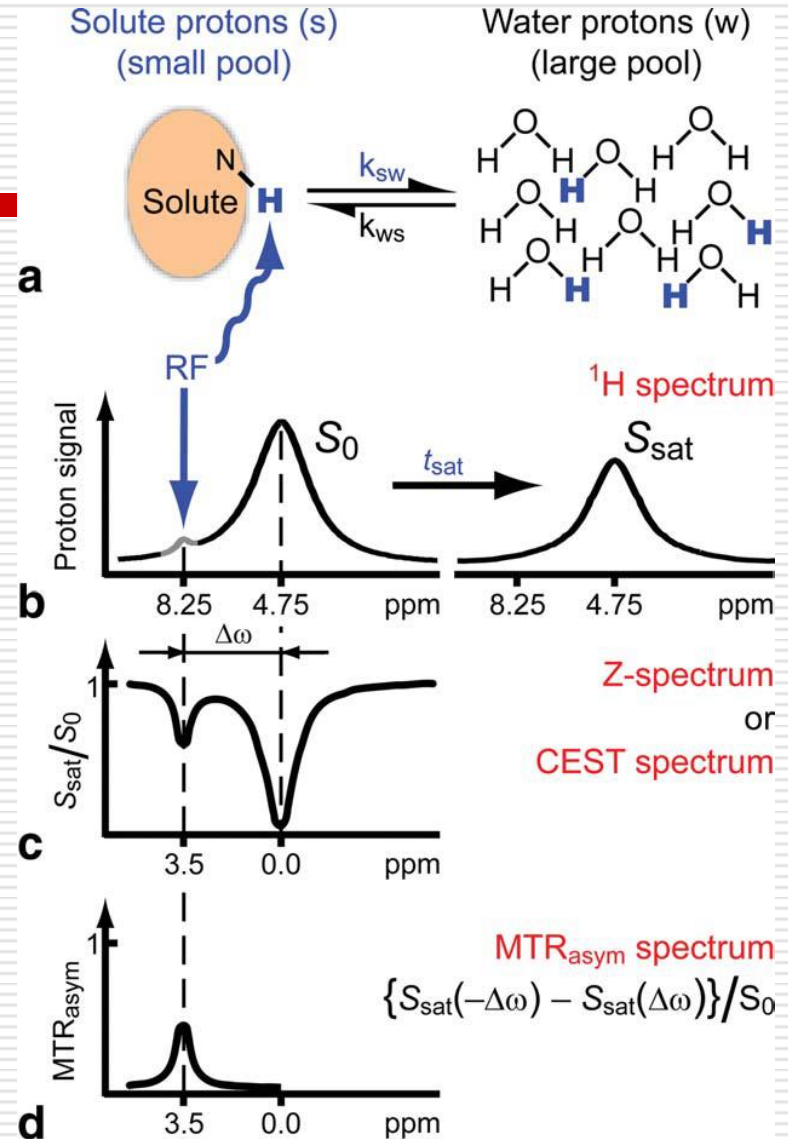


Reproduced from Ward, Aletras & Balaban. *J. Magn. Reson.* **143**: 79 (2000)

# CEST and paraCEST agents prospects for clinical translation

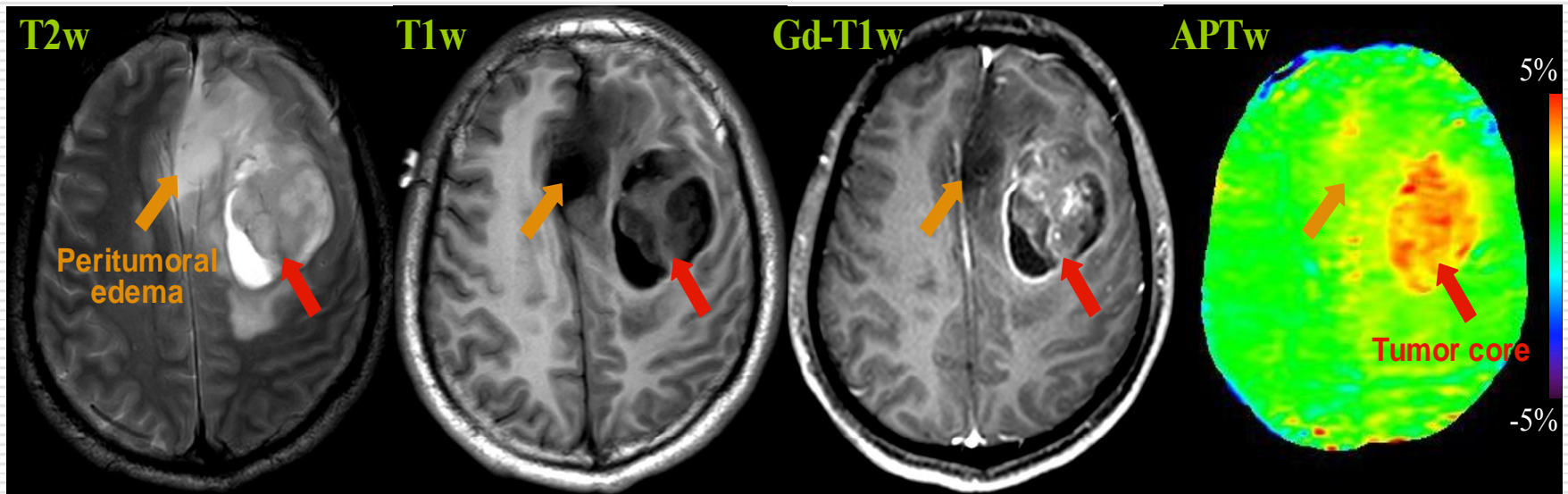
There are many chemical types of exchanging protons in tissue:

- N-H from proteins & amino acids, nucleic acids
- O-H from sugars, polysaccharides
- S-H from cysteine & glutathione
- many others



# Amide Proton Transfer (APT) signal of tumors reflects enhanced -NH proton exchange

Wen, et al., NeuroImage, 51: 616-622 (2010)

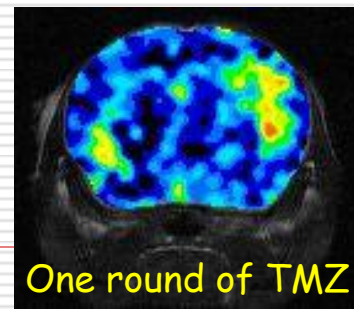
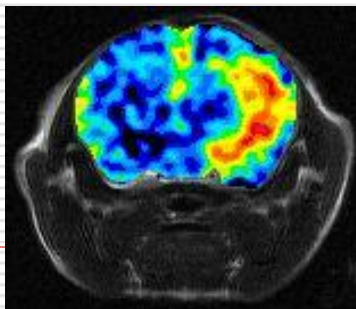
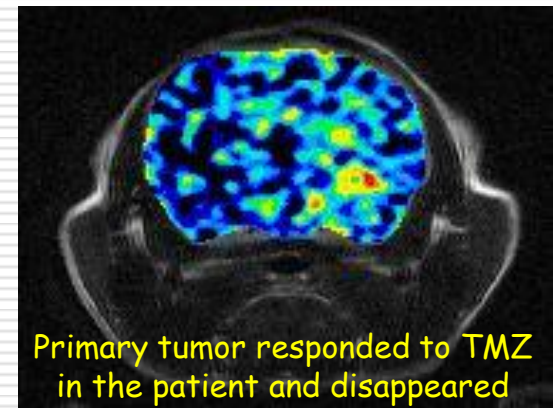
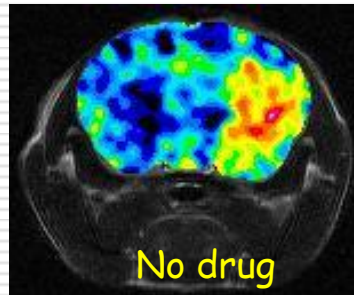
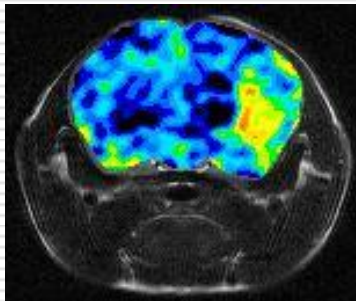
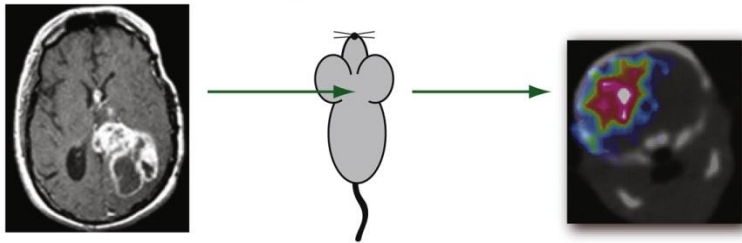


Note: limited contrast in edema region (orange arrow);  
high APT contrast in tumor

# APT imaging detects early response in glioblastoma (GBM) to temozolomide

K. Sagiya, et al., PNAS, 111: 4542-4547 (2014)

Human GBM    Implant cells    Mouse GBM

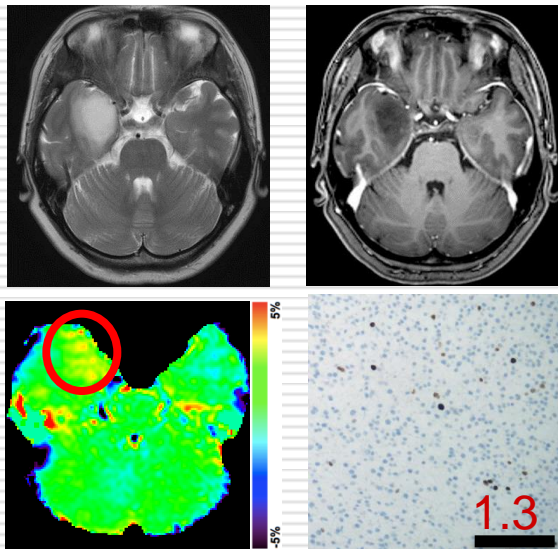




# Amide proton transfer imaging of adult diffuse gliomas: correlation with histopathological grades

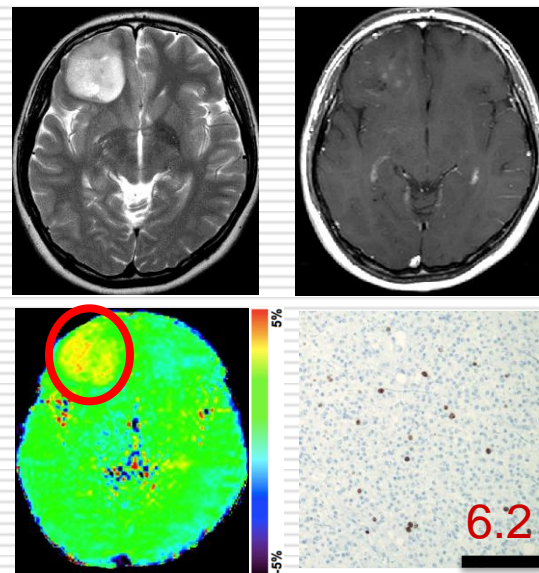
Togao, et al., Neuro-Oncology, 16: 441-448 (2014)

**Astrocytoma  
(Grade II)**



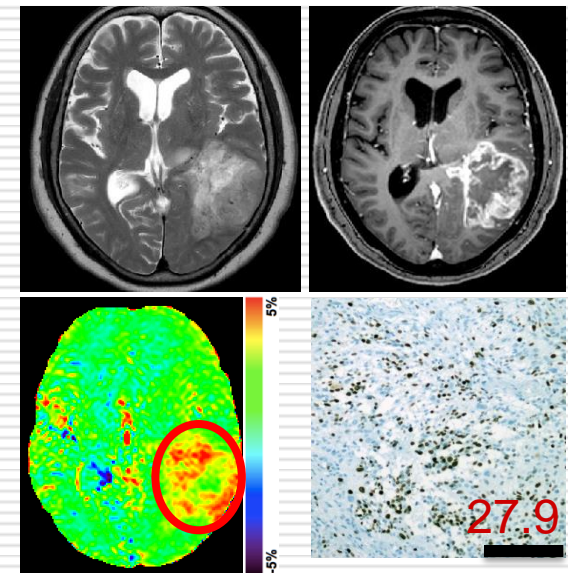
**1.4**

**Anaplastic oligodendroglioma  
(Grade III)**



**2.8**

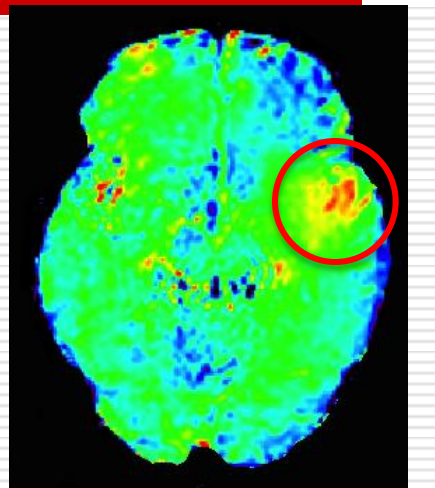
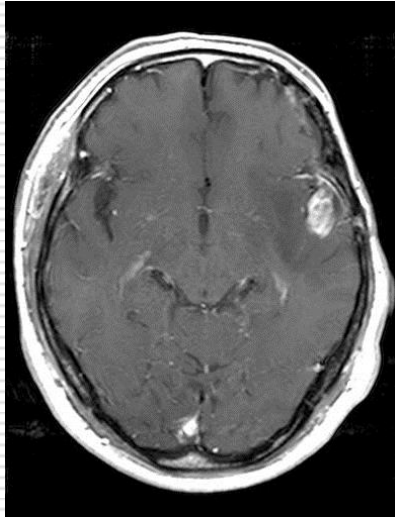
**Glioblastoma multiforme  
(Grade IV)**



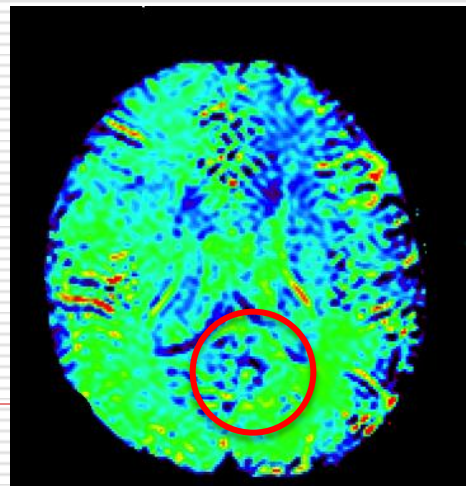
**4.0**

# APT imaging differentiates between tumor recurrence versus radiation necrosis

*By courtesy of Dr. Osamu Togao, Kyushu University*



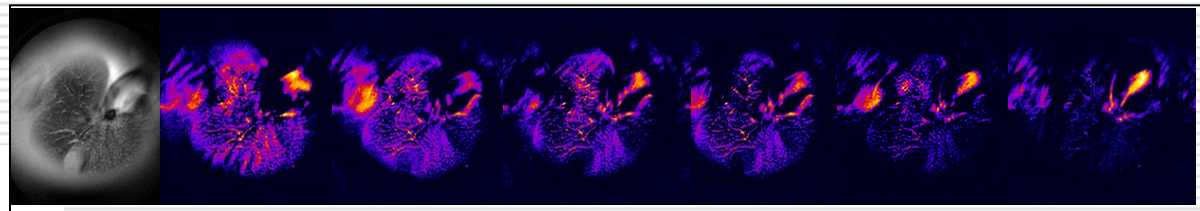
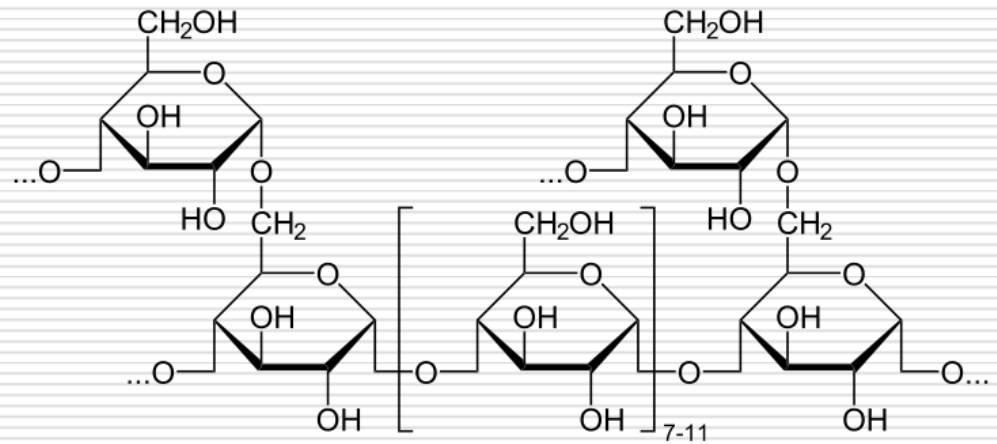
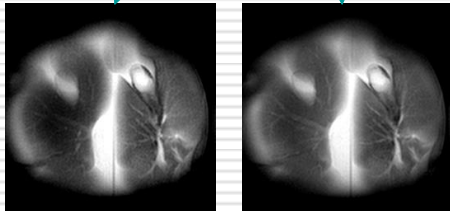
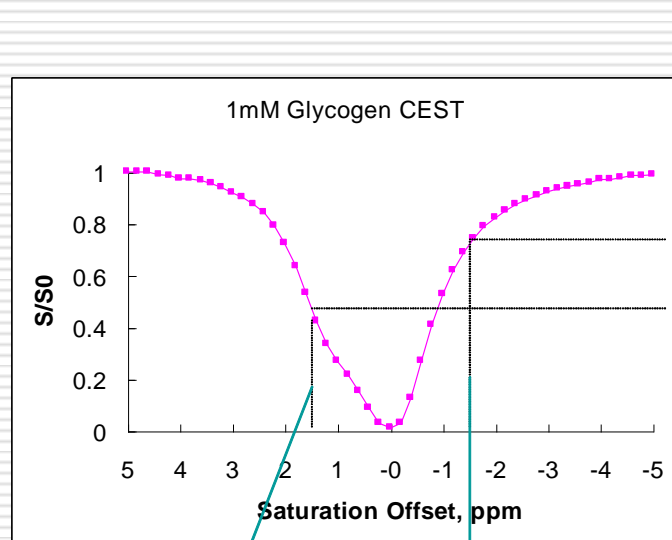
**Recurrence**



**Radiation Necrosis**

# glycoCEST

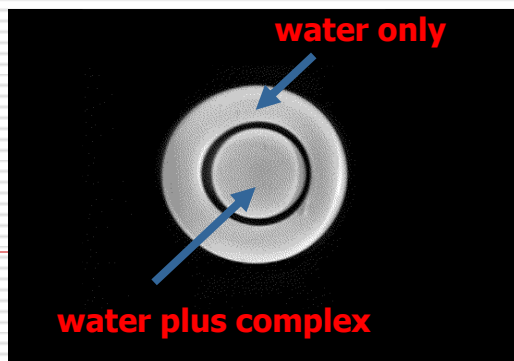
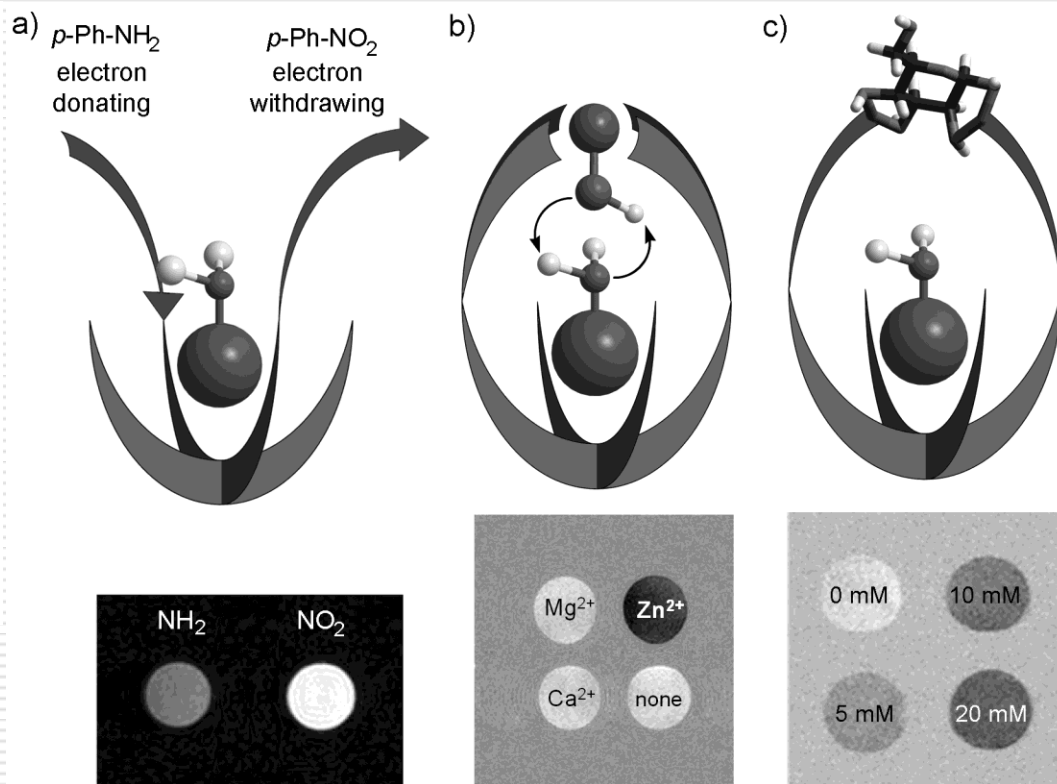
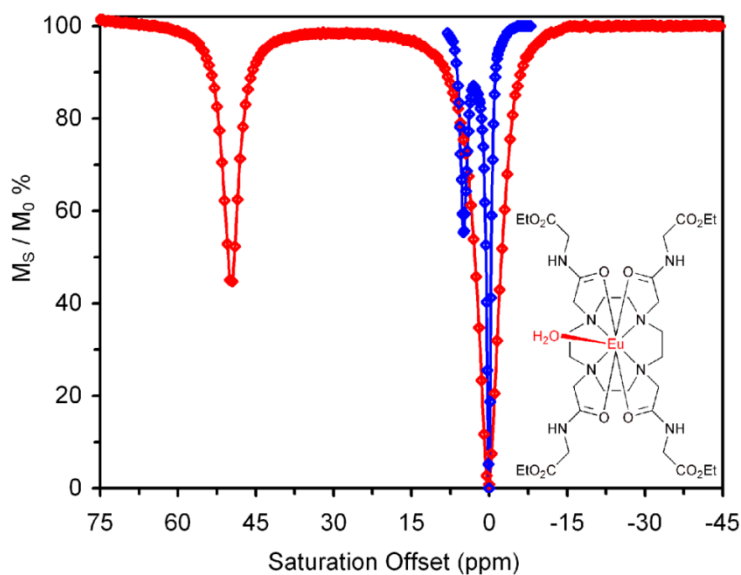
imaging the distribution of glycogen in liver



CEST images showing depletion of glycogen in liver after exposure to glucagon

van Zijl, et al., PNAS, 104, 4359-4364 (2007)

# PARACEST agents can be turned "on" and "off" using frequency-selective RF pulses



The CEST intensity is highly sensitive to water exchange rates  $\Rightarrow$  relatively easy to design responsive agents

---

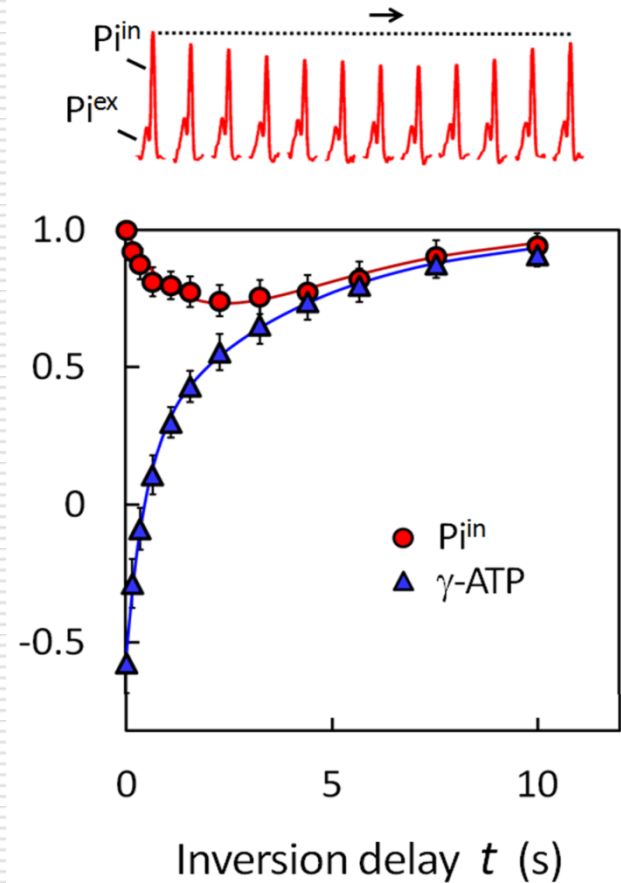
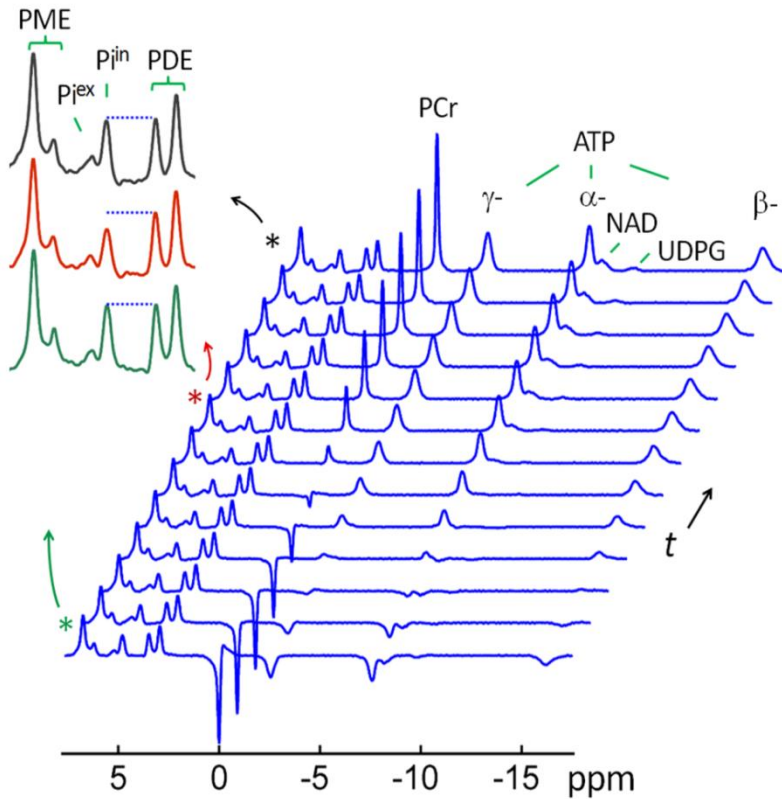
Other lower  $\gamma$  nuclei:  $^{31}\text{P}$ ,  $^{13}\text{C}$  and  $^{23}\text{Na}$

---



# $^{31}\text{P}$ MRS of healthy human brain at 7T

J. Ren, et al., NMR Biomed, 2015, DOI: 10.1002/nbm.3384

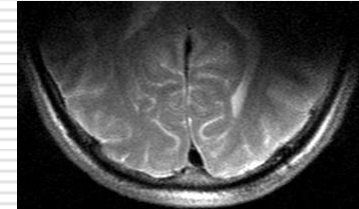


EBIT (Exchange Kinetics by Band Inversion Transfer)

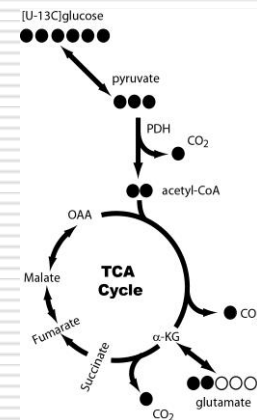
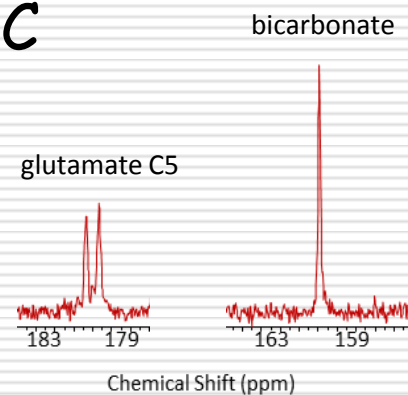
ATP synthesis rate :  $9.9 \pm 2.1$  mmol/min/kg

# $^{13}\text{C}$ is a unique NMR nucleus for probing intermediary metabolism

Nucleus	Spin	Natural abundance	Rel. NMR sensitivity
$^1\text{H}$	1/2	99.9%	100
$^{31}\text{P}$	1/2	100%	6.6
$^{23}\text{Na}$	3/2	100%	9.3
$^{13}\text{C}$	1/2	1.1%	$1.7 \times 10^{-2}$



$^{13}\text{C}$



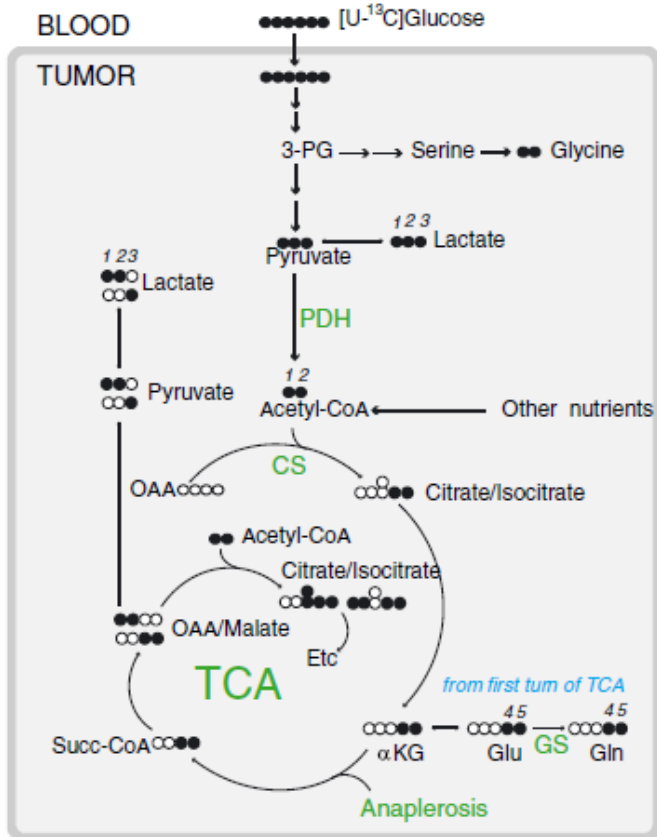
$^{13}\text{C}$  can be used as a tracer of metabolism

- Steady-state  $^{13}\text{C}$  isotopomer methods
- Hyperpolarized  $^{13}\text{C}$  tracers

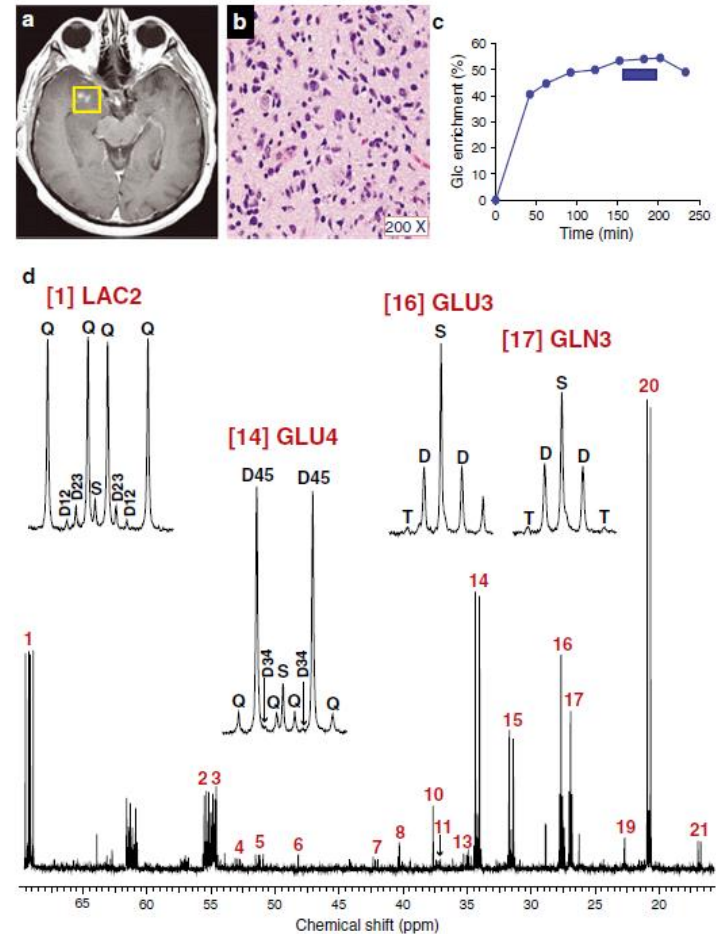


# Metabolism of [U-<sup>13</sup>C<sub>6</sub>]glucose in human brain tumors *in vivo*

EA Maher, et al., NMR in Biomed. 25: 1234-1244 (2012)



Summary of glucose metabolism in tumors. Filled circles represent a carbon with enriched <sup>13</sup>C; open circles reflect <sup>12</sup>C



<sup>13</sup>C NMR spectrum of tumor tissue removed from a patient with a WHO grade II astrocytoma after infusion of [U-<sup>13</sup>C]glucose for 2 hr prior to surgical resection and during removal (8 g/h)

# Summary

---

- MR contrast agents will continue to be useful at higher magnetic fields. Dy-based  $T_{2\text{exch}}$  agents may play a bigger role in imaging biological function at high magnetic fields.
- Responsive MRI contrast agents with high sensitivity can be developed for *in vivo* use, provided that water exchange rates are optimized.  $\text{Zn}^{2+}$  sensitive MRI agents may prove useful for monitoring  $\beta$ -cell function and in detecting prostate tumors.
- CEST & NOE signals from tissues will be greatly magnified at higher magnetic fields. These endogenous contrast mechanisms are sensitive to tissue structures and metabolite contents.
- MRS of lower gamma nuclei will become more important.  $^{13}\text{P}$  NMR will provide ATP synthesis rates from local tissue regions.  $^{13}\text{C}$  NMR will provide metabolic flux details.